Translational control of E2f1 regulates the Drosophila cell cycle

Ovrebo, Jan Inge

2022-01-25

Ovrebo , J I , Bradley-Gill , M-R , Zielke , N , Kim , M , Marchetti , M , Bohlen , J , Lewis , M , van Straaten , M , Moon , N-S & Edgar , B A 2022 , ' Translational control of E2f1 regulates the Drosophila cell cycle ' , Proceedings of the National Academy of Sciences of the United States of America , vol. 119 , no. 4 , e2113704119 . https://doi.org/10.1073/pnas.2113704119

http://hdl.handle.net/10138/353908
https://doi.org/10.1073/pnas.2113704119

Translational control of *E2f1* regulates the *Drosophila* cell cycle

Jan Inge Øvrebø[a,1], Mary-Rose Bradley-Gill[b], Norman Zielke[c], Minhee Kim[b], Marco Marchetti[a], Jonathan Bohlen[d], Megan Lewis[a], Monique van Straaten[d], Nam-Sung Moon[b], and Bruce A. Edgar[a,1]

[a]Huntsman Cancer Institute, Department of Oncological Sciences, University of Utah, Salt Lake City, UT 84112; [b]McGill University, Montreal, QC H3A 0G4, Canada; [c]University of Helsinki, 00014 Helsinki, Finland; and [d]Deutsches Krebsforschungszentrum, 69120 Heidelberg, Germany

Edited by Terry Orr-Weaver, Department of Biology, Whitehead Institute and Massachusetts Institute of Technology, Cambridge, MA; received July 28, 2021; accepted December 10, 2021

E2F transcription factors are master regulators of the eukaryotic cell cycle. In *Drosophila*, the sole activating E2F, E2F1, is both required for and sufficient to promote G1→S progression. E2F1 activity is regulated both by binding to RB Family repressors and by posttranscriptional control of E2F1 protein levels by the EGFR and TOR signaling pathways. Here, we investigate cis-regulatory elements in the *E2f1* messenger RNA (mRNA) that enable *E2f1* translation to respond to these signals and promote mitotic proliferation of wing imaginal disc and intestinal stem cells. We show that small upstream open reading frames (uORFs) in the 5′ untranslated region (UTR) of the *E2f1* mRNA limit its translation, impacting rates of cell proliferation. *E2f1* transgenes lacking these 5′UTR uORFs caused TOR-independent expression and excess cell proliferation, suggesting that TOR activity can bypass uORF-mediated translational repression. EGFR signaling also enhanced translation but through a mechanism less dependent on 5′UTR uORFs. Further, we mapped a region in the *E2f1* mRNA that contains a translational enhancer, which may also be targeted by TOR signaling. This study reveals translational control mechanisms through which growth signaling regulates cell cycle progression.

E2F1 | translational control | uORF | cell cycle | TOR

Postembryonic cell proliferation is controlled largely by extracellular signaling and nutrients that stimulate both growth-associated (anabolic) metabolism and cell cycle progression. However, despite great progress in understanding both cell signaling and cell cycle regulation, the mechanisms that link growth signaling to the cell cycle control apparatus remain poorly understood. Studies in yeast have led to models in which cell proliferation is a direct consequence of cell growth, either through dilution of a cell cycle inhibitor as cell volume increases or, alternatively, through growth-dependent accumulation of cell cycle activators (1–3). In budding yeast, the level of Cln3, a G1 cyclin analogous to metazoan Cyclins D and E, are highly sensitive to translational efficiency. *Cln3* possesses a short upstream open reading frame (uORF) that dampens *Cln3* translation, favoring accumulation when overall translational efficiency is high (2). Because Cln3 activity is rate-limiting for G1/S progression, manipulation of Cln3 synthesis rates affects the size at which yeast cells divide. Similarly, M-phase entry is regulated by translation rates in fission yeast, where translation of a limiting mitotic activator, Cdc25, is highly sensitive to cellular translation rate (4). Another study demonstrated that subthreshold concentrations of Whi5, a negative cell cycle regulator, are sufficient to trigger G1/S (1). Because the amount of Whi5 per cell is constant throughout G1, cell volume increases during G1 are sufficient to dilute Whi5 to levels that allow G1/S entry. These different mechanisms are not mutually exclusive but rather reflect the likely possibility that metazoan cell cycles harbor multiple growth-sensing mechanisms to ensure that division is tightly coordinated with cell growth.

The involvement of a growth responsive cell cycle regulator, i.e., a "growth sensor," is a shared feature of these models from yeasts, but such a mechanism has so far not been elaborated in metazoan cells. Current models of the metazoan cell cycle do not include specific explanations for why cells enter the cell cycle only once a certain cell volume or growth rate is achieved, though this topic is widely discussed (3, 5, 6). In textbook models of mammalian cell cycle control, growth factor signaling triggers a transcriptional cascade that culminates in the expression of Cyclin D (CycD1, D2, D3), the activator of Cyclin Dependent Kinases 4 and 6 (Cdk4, Cdk6). CycD/Cdk4 complexes then phosphorylate Retinoblastoma protein (Rb) family transcriptional repressors to unleash E2F family transcriptional activators that promote transcription of a large set of genes needed for DNA replication and mitosis (7–9). However, whether this model can be universally applied is debatable, as several studies report examples wherein Cyclin D and/or CDK4/6 are dispensable for cell proliferation (10–12), and show that cells are responsive to growth factor signaling in their absence. While extensive data support the importance of the E2F transcriptional activators for cell cycle progression, there are probably unknown factors in addition to Rb repressors that control E2F activity.

Previous work in *Drosophila* indicates that E2F1 acts as a potential growth sensor during G1→S transitions in endocycling salivary gland cells and midgut enterocytes. In *Drosophila*'s

Significance

Here, we explore a mechanism wherein the growth signaling-dependent translation of mRNA encoding a cell cycle regulatory factor limits rates of cell proliferation. An essential cell cycle transcription factor, E2F1, was found to be post-transcriptionally regulated by TOR and EGFR signaling, and thus served as a candidate growth sensor for this study. Using expression of green fluorescent protein (GFP)-E2F1 transgenes with alterations within the *E2f1* 5′ untranslated region (UTR), we altered the translation of GFP-E2F1 and changed cell proliferation rates accordingly. Further, we found that 5′UTR upstream open reading frames are TOR-sensitive regulatory components of *E2f1* translation. Our observations indicate that growth signaling dependent protein translation is an important regulator of cell proliferation.

Author contributions: J.I.Ø., N.Z., N.-S.M., and B.A.E. designed research; J.I.Ø., M.-R.B.-G., N.Z., M.K., M.M., J.B., M.L., and M.v.S. performed research; J.I.Ø. contributed new reagents/analytic tools; J.I.Ø., M.-R.B.-G., N.Z., M.M., N.-S.M., and B.A.E. analyzed data; and J.I.Ø. and B.A.E. wrote the paper.

The authors declare no competing interest.

This article is a PNAS Direct Submission.

[1]To whom correspondence may be addressed. Email: jan.ovrebo@uib.no or bruce.edgar@hci.utah.edu.

This article contains supporting information online at http://www.pnas.org/lookup/suppl/doi:10.1073/pnas.2113704119/-/DCSupplemental.

Published January 24, 2022.

salivary glands, E2F1 protein levels are posttranscriptionally regulated by the TOR signaling pathway (13), whereas in adult midgut enterocytes, levels of E2F1 protein, but not messenger RNA (mRNA), were found to be EGFR/RAS-dependent (14). TOR activity is regulated by nutrient-dependent Insulin/PI3K signaling and amino acid levels and can increase translational efficiency by stimulating factors including S6K and eIF4E (15–18). TOR thus provides a link between nutritional sensing and translation. The translational efficiency of mRNAs is greatly influenced by the sequence and structure of their 5′ untranslated regions (UTR), which can suppress or enhance translation initiation. uORFs in the 5′UTR cannot only suppress translation but can also favor translation of select transcripts during cellular stress (19). A well-known example is the stress-activated translation of mammalian ATF4. In this case, the eukaryotic Initiation Factor 2 (eIF2) is phosphorylated upon stress, and this reduces the number of eIF2 ternary complexes and the ability of uORFs to throttle translation of ATF4. There is also a known mechanism wherein uORFs can be selectively bypassed to allow translation in nonstressed conditions. In *Drosophila*, DENR and MCT-1 can promote reinitiation of ribosomal scanning along the 5′UTR, thus aiding the ability of ribosomes to reinitiate translation at start codons downstream of a uORF (20). Shortening of 5′UTRs, and thus removal of uORFs, can increase translation in both mammalian and *Drosophila* cells (21, 22). Furthermore, secondary RNA structures in 5′UTRs, including 5′ Terminal Oligo-Pyrimidine tracts and stable hairpin structures, can also influence the translational efficiency of an mRNA. These structures are especially dependent upon the RNA helicase activity of eIF4E (23–25), which can be controlled by TOR through phosphorylation of the eIF4E inhibitor, 4E-BP. In addition, TOR also activates another RNA helicase responsible for "melting" secondary structures, eIF4B, through activation of S6K. In conclusion, mRNA translation can be selectively regulated in response to growth conditions, and such a mechanism is likely to impact the levels and activities of cell cycle regulators, thus linking the cell cycle apparatus to cell growth. Here, we further investigate the function of *Drosophila* E2F1 as a translationally regulated growth sensor. Our studies indicate that uORFs and a ∼400 nucleotide region within the 5′UTR have significant regulatory effects on *E2f1* translation and on E2F1-dependent cell proliferation.

Results

***E2f1* Expression Is Regulated Posttranscriptionally by TOR in Mitotic Cells.** Our previous work demonstrated that *Drosophila E2f1* is posttranscriptionally regulated by EGFR/Ras/Raf and TOR signaling in adult midgut enterocytes and larval salivary gland cells, respectively (13, 14). Both cell types are postmitotic, polyploid endocycling cells. *E2f1* has also been reported to be posttranscriptionally up-regulated by TSC/TOR in diploid mitotic cells of the *Drosophila* eye disc (26), although whether this up-regulation affected proliferation was not tested. In wing imaginal discs (WD), overexpressed E2F1 accelerates proliferation and loss of E2F1 arrests proliferation (27), indicating that E2F1 levels can be rate-limiting for mitotic cell cycle progression. We therefore tested whether E2F1 levels are posttranscriptionally regulated by TOR and/or EGFR signaling in WD cells. To do this, we overexpressed Rheb, an activator of TOR (28), or activated Ras ($Ras^{V12,S35}$) (29), or their downstream targets, Myc and S6K, in the posterior WD. We then compared E2F1 levels in posterior versus anterior WDs using an anti-E2F1 antibody (30). We observed that overexpressed Rheb increased E2F1 protein expression (Fig. 1 *A* and *B*) without affecting *E2f1* mRNA levels (Fig. 1*C*). Using the same approach, we also observed increased *E2f1* expression following Myc or $Ras^{V12,S35}$ overexpression (*SI Appendix*, Fig. S1), though no significant change was observed following overexpression of a constitutively active form of S6K ($S6K^{TE}$) (31), a downstream effector of TOR. Thus, Myc and $Ras^{V12,S35}$ promoted E2F1 protein expression in WDs but to a lesser extent than Rheb (Fig. 1*B*). TOR is known to regulate general translation through S6K activation in growing cells (15–18). These results demonstrate that TOR is also likely to regulate E2F1 protein levels posttranscriptionally in mitotic cells, a relationship similar to that reported earlier in endocycling cells (13). However, we cannot exclude the possibility that TOR also influences *E2f1* expression through transcription, for instance, through affecting *E2f1* isoform expression. Both TOR and Ras activity can promote cell growth and G1→S transitions in WD cells (28, 32), and it has also been demonstrated that *E2f1* expression limits cell cycle progression in these cells (27). Thus, our results suggest that TOR signaling promotes WD cell cycle progression by posttranscriptionally increasing E2F1 protein levels through a mechanism independent of S6K.

***E2f1* Translation Rate Is Controlled by Its UTRs.** We hypothesized that posttranscriptional control of E2F1 levels might be executed by translational control sequences in the *E2f1* mRNA. Hence, we tested whether the translation of *E2f1* mRNA is dependent on sequences in its UTRs. mRNA translation is often regulated through 5′UTRs, which can contain linear motifs and secondary structures that interfere with translation initiation (33–38). Interestingly, the predicted *E2f1* mRNA isoforms include six variant 5′UTRs and one alternative transcription termination site that gives rise to two variant lengths of the 3′UTR (Fig. 1*D* and *SI Appendix*, Fig. S2) (39) (FlyBase version FB2021_3). Two variant isoforms of the E2F1 protein have also been reported, such that one variant, E2F1b, possesses an additional short (48bp) internal exon, adding 16 amino acids to a region of the E2F1 sequence known as the "marked box domain" (40). Expression of both E2F1 protein isoforms is required to sustain larval development and endocycles, where E2F1b is especially required in salivary glands. Based on isoform analysis of RNA sequencing data using the Cufflinks algorithm, the *E2f1-RA* mRNA isoform was found to be the predominant isoform expressed in S2R+ cells, WDs, and salivary glands (Fig. 1*E*). This isoform possesses the longest 5′UTR, which contains an unusually high number (11 in total) of conserved short uORFs for *Drosophila* (Fig. 1*F* and *SI Appendix*, Fig. S3) (41). A shorter *E2f1* isoform, *E2f1-RE*, was the predominant isoform expressed in cells of the adult midgut, which includes intestinal stem cells (ISCs), enteroblasts (EBs), and enterocytes (Fig. 1*E*). To test the potential functions of elements in the *E2f1* 5′UTRs we designed a translational sensor assay that allowed us to compare the translational efficiency of sensors containing different UTR sequences *in vivo*. These sensor mRNAs possess a green fluorescent protein (GFP) coding sequence (CDS) flanked by a 5′UTR and 3′UTR from either *E2f1* or β-globin (*SI Appendix*, Fig. S4*A*). A short *Xenopus* β-globin UTR was chosen as a control due to its lack of known regulatory sequences (42). The CDS contains a super folder GFP, a nuclear localization signal, and *Escherichia coli* dihydrofolate reductase (ecDHFR). These sensors were expressed in S2R+ cells under control of an actin promoter. The ecDHFR CDS destabilizes expressed proteins through recognition by the proteasome unless bound to Trimethoprim, a small molecule that can be added to the cells to control sensor expression (43). S2R+ cells were imaged for 24 h, with or without the addition of Trp at T = 0 h, on an Olympus ScanR Screening Microscope. We observed that the translational sensor with the full-length *E2f1* UTR sequences (RA) accumulated GFP more slowly than a sensor possessing short UTRs (ΔUTR; Fig. 1*G*). This indicated that the *E2f1-RA* UTRs possess regulatory sequences that attenuate *E2f1* expression in S2R+ cells. mRNA levels were not affected by the different

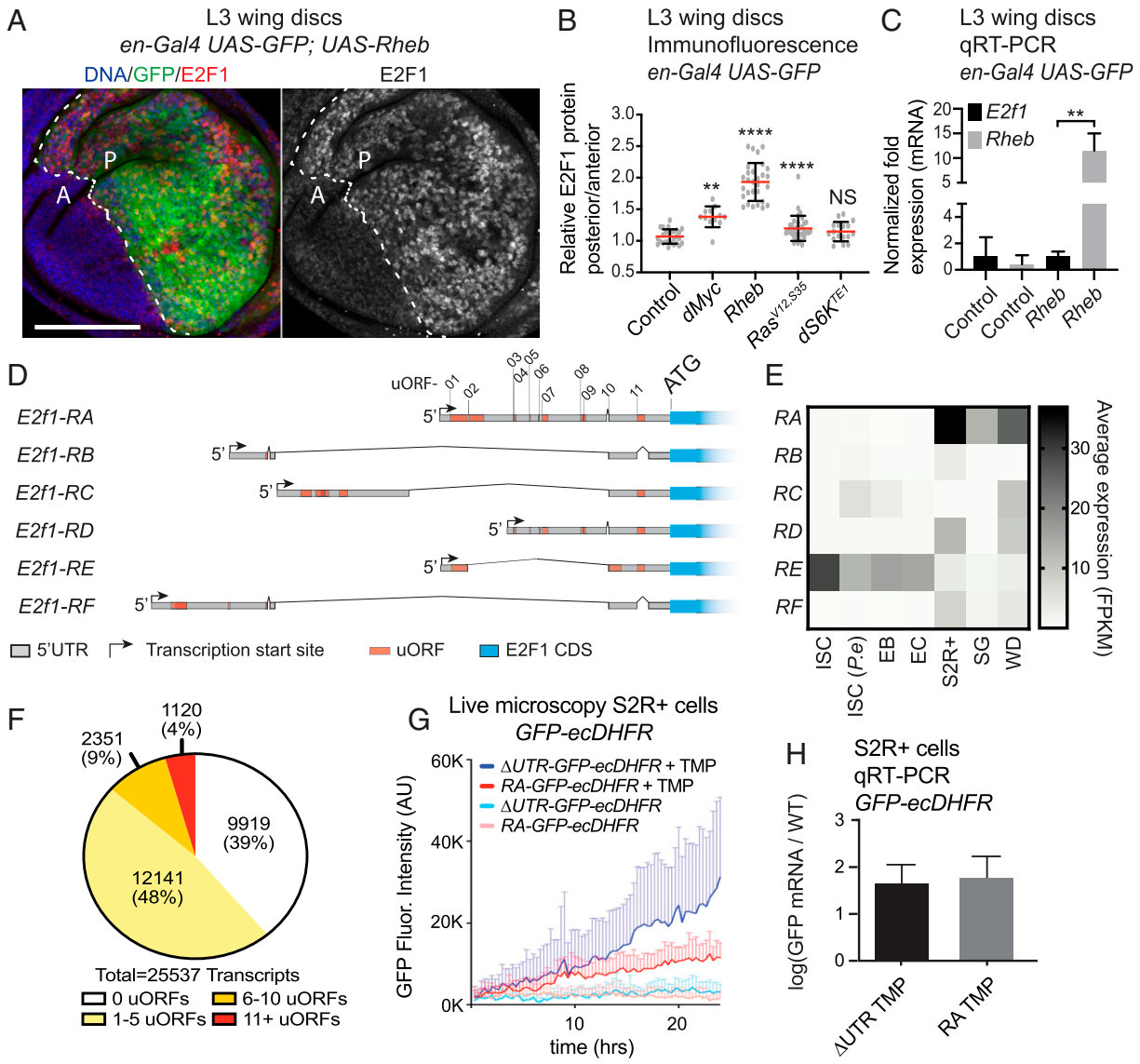

Fig. 1. *E2f1* expression is posttranscriptionally regulated through its 5′UTR in *Drosophila* imaginal discs. (*A*) *Myc*, *Rheb*, $Ras^{V12,S35}$, and $S6K^{TE1}$ were overexpressed in the posterior WD (P) using the *engrailed* driver. E2F1 levels, stained with anti-E2F1 antibody, were enriched in cells overexpressing Rheb. (Scale bar: 100 μm.) (*B*) Quantification of posterior E2F1 levels relative to anterior E2F1 levels in WDs. Overexpression of *Myc*, *Rheb*, and Ras^{V12S35} induced increased expression of E2F1 in posterior WD compared to control cells in the anterior (A) WD. (*C*) qRT-PCR of *E2f1* and *Rheb* mRNA levels in WT WDs and discs overexpressing *Rheb*. (*D*) *Drosophila E2f1* has six isoforms differing mainly by alternative splicing of the 5′UTR. (*E*) RNAseq expression data of *E2f1* isoform transcripts from ISCs, EBs, enterocytes (ECs), salivary glands (SG), WDs, and S2R+ cells. (*F*) Distribution of uORFs in *Drosophila* transcripts. Graph based on published data (41). (*G*) Live recording of fluorescence accumulation, generated from *E2f1* translational sensors, in S2R+ cells. *RA-E2F1* translational sensor displays lower accumulation rate compared to ΔUTR sensor. (*H*) qRT-PCR analysis of expressed translational sensors reveals no significant effect on mRNA levels. Error bars in *B* and *H* represent mean and SD. Student's *t* test performed in *B* and *H* (*$P > 0.05$, **$P > 0.01$,***$P > 0.001$, ****$P > 0.0001$).

UTRs (Fig. 1*H*), implying that UTRs regulate expression by altering translation efficiency.

The 5′UTR of the *E2f1-RA* Isoform Encodes a TOR-Responsive Element. As shown in Fig. 1, E2F1 protein expression is responsive to TOR activity in imaginal discs. To test whether TOR-responsive elements might be present in the 5′UTR of the *E2f1-RA* mRNA, we induced clones of $Tsc1^{-/-}$ cells, which have high TOR activity, in eye discs carrying mutations of the *E2f1* 5′UTR RD/RA/RE region (44) (*SI Appendix*, Fig. S2). The $E2f1^{\Delta RA}$ mutant has had the entire RD/RA/RE region removed by FLP-FRT recombinase using two flanking FRT sites (44). Another allele, $E2f1^{RS5}$ ($P\{RS5\}E2f1^{5\text{-}HA\text{-}1661}$), possesses an RS5 P-element insertion (45, 46) that has previously been shown to primarily affect expression of the *E2f1-RE*, *RA*, and *RD* isoforms (44, 46). We found that E2F1 levels were markedly increased in $Tsc1^{-/-}$ clones that were wild type for *E2f1* but were not increased in cells that were also homozygous for either $E2f1^{RS5}$ or $E2f1^{\Delta RA}$ (Fig. 2 *A* and *B*). *E2f1* transcripts were not enriched in *Tsc1* mutants compared to control, indicating that E2F1 protein levels are increased posttranscriptionally in *Tsc1* mutants (Fig. 2*C*). qRT-PCR of $E2f1^{\Delta RA}$ and $E2f1^{RS5}$ (44) mutant eye discs revealed that the total *E2f1* mRNA levels were only mildly affected (Fig. 2*D*, *Left* bars), suggesting the *E2f1* RB, RC, and RF mRNA isoforms are incapable of responding to increased TOR activity. This suggests that TOR regulates expression of E2F1 protein levels posttranscriptionally through a feature unique to the *E2f1-RA*, *-RD*, and *-RE* mRNAs.

uORFs Limit *E2f1* Translation in Wing Discs. Next, we tested whether certain UTR sequences are sufficient to control *E2f1* translation and proliferation in vivo. We therefore constructed a panel of transgenes possessing alterations in the *E2f1* UTR sequences (Fig. 3*A*) to use for in vivo expression tests. We investigated the *E2f1-RA* isoform because it possesses the longest 5′UTR among the 6 *E2f1* mRNA isoforms and because it is the predominant isoform expressed in larval tissues (salivary glands, WDs) and also in S2R+ cells (Fig. 1*E*). We included the longer 3′UTR variant because the length of the 3′UTR is modified during transcription by the presence of alternative polyadenylation sites (47, 48). Our alterations in the *E2f1-RA* 5′UTR included 5 nested truncations [Δ(1-414), Δ(207-621), Δ(414-828), Δ(621-1035), Δ(828-1242)] and a variant with single nucleotide substitutions (ATG→AAG) to remove all 11 uORF start codons (ΔuORF) (Fig. 3*A* and *SI Appendix*, Fig. S4*B*). To measure effects on mRNA translation without affecting the cell cycle, we constructed one set of transgenic lines, referred to henceforth as "translational sensors," which included the GFP protein CDS but not the *E2f1* CDS (*SI Appendix*, Fig. S4*C*). The *E2f1* CDS was excluded in these constructs to prevent periodic degradation normally conferred by the E2F1 PIP degron (49) as well as changes in proliferation that might affect GFP accumulation. The translational sensors were expressed in WDs using the Gal4/UAS expression system (50). Gal4 was expressed in entire larvae using the *tubulin* promoter (tubGal4). Larvae expressing the translational sensors were raised at 25 °C for 6 d until the wandering L3 stage. We confirmed by qRT-PCR that the sensor mRNAs were expressed at similar levels, suggesting that changes in the 5′UTR did not influence the amount of available mRNA (Fig. 3*B*). GFP levels of individual WD cells from ∼20 WDs were then measured by flow cytometry using Hoechst 33342 to identify nucleated cells (*SI Appendix*, Fig. S5*A*). We observed that inactivating the uORFs strongly increased the levels of GFP compared to the control construct (Fig. 3*C*). A similar increase in GFP expression induced by a construct based on the *E2f1-RD* isoform (*RD-GFP*), lacking uORFs ($RD^{\Delta uORF}$-*GFP*) (*SI Appendix*, Fig. S4*C*), was also detected in eye discs (*SI Appendix*, Fig. S6 *A*–*C*). These results are consistent with uORFs acting as a translational throttle (51). Three transgenes possessing deletions in the 5′UTR [Δ(1-414), Δ(207-621), and Δ(621-1035)-GFP] expressed levels of GFP that were higher than RA-GFP but lower than ΔuORF-GFP. Each of these deletions removed 3 to 5 uORFs, which may explain the increased GFP levels. Two transgenes, Δ(414-828) and Δ(828-1242), expressed decreased GFP levels compared to the RA-GFP control transgene (Fig. 3*C*), suggesting that sequences in the 414-828 and 828-1242 regions enhance translation of *E2f1* mRNA. The Δ828-1242 truncation covers a region found in the 5′UTR of all *E2f1* isoforms, whereas the Δ414-828 truncation covers a region present only in the RA and RD mRNA isoforms.

A possible mechanism to explain these results is that this region serves as an internal ribosomal entry site (IRES), which allows ribosomes to bypass a majority of the uORFs. We therefore constructed a bicistronic translational sensor similar to the RA-GFP translational sensor but containing an RFP CDS insertion at the 414 nt position ($RA\text{-}RFP^{414}\text{-}GFP^{NLS}$, *SI Appendix*, Fig. S4*C*). IRES activity should thus be detected by the presence of GFP signal. When expressed in larval WDs, we could not detect GFP, suggesting *E2f1* is not controlled through this mechanism in this tissue (*SI Appendix*, Fig. S7). However, we could detect GFP signal in salivary glands, suggesting an IRES may facilitate *E2f1* translation in a tissue-dependent manner. We also observed GFP expression in a few cells (<5 GFP+ cells per gut) of the adult midgut. We conclude that 5′UTR uORFs limit the translation rate of *E2f1* and that the (414-828) and (828-1242) regions are required for optimal translation of *E2f1* through a mechanism independent of IRES in larval WDs. Interestingly, the (621-1035) deletion, which overlaps with the (414-828) and (828-1242) region, did not display decreased translation. This result may suggest the presence of multiple regulatory sites in this region, such that different combinations of deleted sites yields different effects. It could also be the consequence of alterations in an RNA tertiary structure that dictates translation efficiency.

Mitotic Cell Cycle Rate Is Regulated by *E2f1* Translation. Expression of E2F1 has previously been shown to be rate-limiting for endocycling in the salivary glands and was proposed to act as a sensor of growth and growth signaling (i.e., TOR activity) in that tissue (13). To determine whether *E2f1* translation rates also control rates of proliferation in mitotic cells, we performed experiments in larval WDs. To test whether cell cycle rates can be adjusted by the rate of *E2f1* translation in larval WDs, we expressed transgenes with 5′UTR alterations identical to those used in the translational sensors described previously but encoding a functional GFP-E2F1 (Fig. 3*A* and *SI Appendix*, Fig. S4*B*). We crossed these transgenes with an *engrailed*-Gal4 driver line coexpressing temperature sensitive Gal80 (*en-Gal4 tub-Gal80^{ts}*) so that ectopic GFP-E2F1 expression would be limited to posterior wing compartments after a temperature shift. GFP^{+} offspring were raised for 5 d at 18 °C and shifted to 29 °C to activate GFP-E2F1 expression 2 d before dissection. Live WD cells were dissociated, stained for DNA and run through a flow cytometer (Cytoflex). We noticed a significantly increased ratio of cell numbers in the posterior wing compartment compared to anterior wing compartment when overexpressing E2F1 transgenes, with the exception of the Δ*(414-828)-E2F1* and Δ*(828-1242)-E2F1* transgenes (Fig. 3*D*), which had normal cell numbers. This is consistent with the very low rate of translation of these two transgenes (Fig. 3*C*). We also observed decreased cell sizes in E2F1-overexpressing cells, and we noticed that cells expressing Δ*(207-621)-E2F1* were significantly smaller than *RA-E2F1* expressing cells, while Δ*(414-828)-E2F1* expressing cells were larger (Fig. 3*E*). However, the strongly expressed Δ*uORF-E2F1* transgene displayed a lower cell number ratio than the *RA-E2F1* control (Fig. 3*D*), suggesting that E2F1 cannot increase proliferation if expressed beyond a certain level. It is also known that excessive *E2f1* expression causes apoptosis. Indeed, we observed more apoptosis when expressing the strongly translated Δ*uORF-E2F1* transgene compared to the more weakly expressed *RA-E2F1 transgene* (Fig. 3*F*). We then asked how different levels of *E2f1* translation affected cell cycle progression. We therefore compared DNA profiles to assay the proportions of cells in G1, S, and G2 phase (Fig. 3*G*). We compared three transgenes representing three levels of translation efficiency: Δ*(414-828)-E2F1* (low translation), *RA-E2F1* (medium translation), and Δ*(1-414)-E2F1* (high translation). We found that higher levels of *E2f1* expression correlated with decreased numbers of G1 cells and increased numbers of G2 cells (Fig. 3*G*). These data, which are consistent with an earlier analysis of E2F1 function in WDs in Ref. 27, demonstrate that alterations in *E2f1* translation, mediated through its 5′UTR, alter cell size and G1 length in a rate-limiting manner in mitotic cells.

uORFs Render *E2f1* Translation Sensitive to TOR. As demonstrated previously, *E2f1* translation is sensitive to TOR activity in WDs (Fig. 1) and salivary glands (13). Thus, we tested whether uORFs or the 414–828 region of the *E2f1* 5′UTR affected sensitivity to TOR activity. We expressed the RA-GFP and ΔuORF-GFP translational sensors in larval tissues using the *tub-Gal4* driver. We then fed early third instar larvae (4 d after egg laying) 100 μM rapamycin for 24 h before WDs were removed by dissection. Larvae fed an equal concentration of dimethyl sulfoxide (DMSO; vehicle) served as controls. GFP fluorescence was measured by flow cytometry (Fig. 4*A* and *SI Appendix*, Fig. S5*A*).

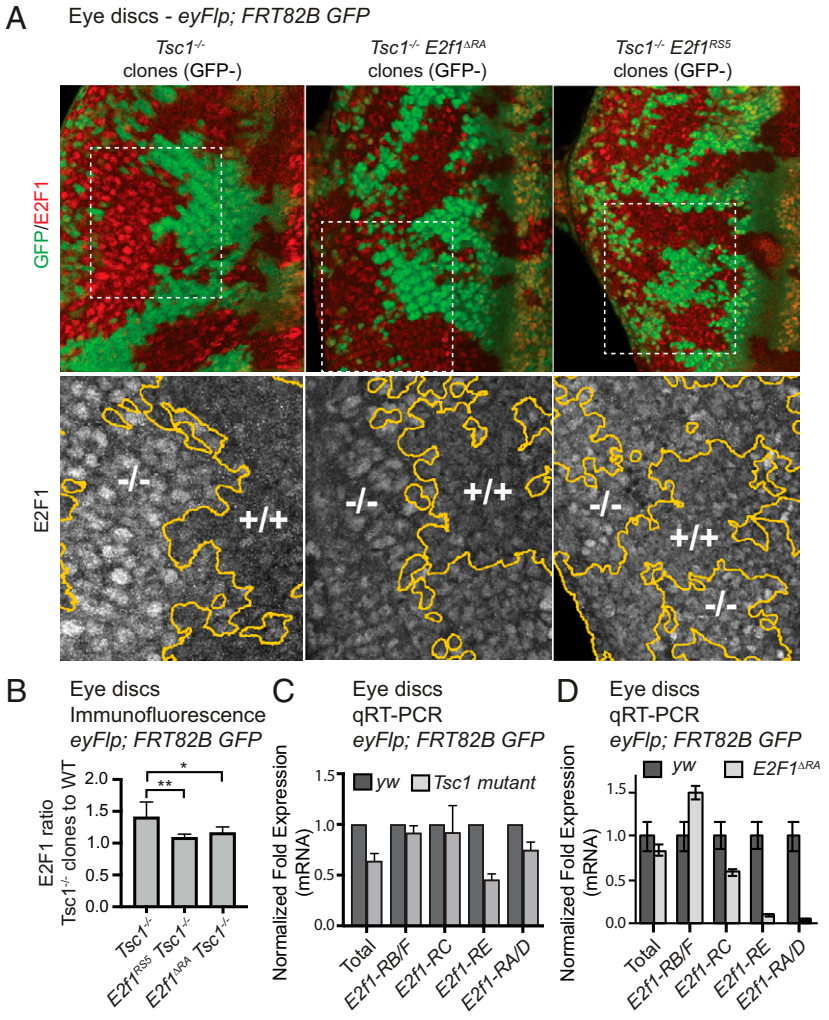

Fig. 2. *E2f1-RA* mRNA possesses a TOR-responsive element. (*A*) FRT-mediated mitotic recombination was used to induce clones homozygous for $Tsc1^{Q87X}$, $Tsc1^{Q87X}$ $E2f1^{\Delta RA}$, or $Tsc1^{Q87X}$ $E2f1^{RS5}$ in heterozygous eye discs. Homozygous cell clones were negatively marked by absence of GFP. E2F1 levels, stained with anti-E2F1 antibody, are enriched in $Tsc1^{-/-}$ clones, but $Tsc1^{-/-}$ clones failed to increase E2F1 expression if the cells were also homozygous for $E2f1^{\Delta RA}$ or $E2f1^{RS5}$. (*B*) Quantification of E2F1 protein levels in mutant clones compared with WT clones. (*C*) qRT-PCR of relative *E2f1* mRNA isoform levels in *Tsc1* mutants. (*D*) qRT-PCR of relative *E2f1* isoform mRNA transcript levels in $E2f1^{\Delta RA}$ mutants.

Because TOR activity regulates cell growth, we used cell size (forward scatter) as a control for successful TOR inhibition (Fig. 4*B*). As expected, GFP fluorescence was weaker in flies expressing RA-GFP and fed rapamycin, demonstrating that suppression of TOR activity suppresses *E2f1* translation. However, WDs expressing ΔuORF-GFP were resistant to rapamycin, suggesting that TOR activity may bypass the suppression of translation by the uORFs (Fig. 4*A*). Next, we tested whether Δ*uORF-E2F1* could maintain proliferation in larvae fed 100 μM rapamycin for 20 h. *RA-E2F1* and Δ*uORF-E2F1* were expressed for 24 h using the *en-Gal4^{ts} UAS-GFP* driver. Dissected WDs were fixed and stained with anti–phosphoserine-10-Histone-H3 (pH3) antibodies to assay mitoses. By assaying proliferation in posterior WDs, we observed strong reduction of *RA-E2F1* driven proliferation (~75% reduction) upon rapamycin treatment, reaching levels similar to anterior control compartments (Fig. 4*C*). However, Δ*uORF-E2F1* was still capable of maintaining high levels of proliferation, with only ~39% reduction (Fig. 4 *C* and *D*), suggesting the Δ*uORF-E2F1* transgene is less dependent on TOR activity. Considering that Δ*uORF-GFP* translation was unaffected by rapamycin treatment, it is likely that the 39% reduction in proliferation is caused by reduced translation of other protein targets that promote cell cycle progression. In conclusion, our data suggest that the presence of uORFs in the *E2f1* 5′UTR render *E2f1* translation more dependent on TOR activity.

***E2f1* Translation Controls ISC Proliferation.** As *E2f1* translation can adjust cell cycle length in wing imaginal cells, we tested whether this is the case in other cell types. Cells of the wing grow and divide continuously through larval development, and we were curious whether *E2f1* translation could determine proliferation/quiescence decisions in cells that proliferate less frequently. We therefore tested E2F1-dependent proliferation in ISCs of the adult midgut, which have long periods of quiescent punctuated by bursts of proliferation, for instance, during damage-induced regeneration following a bacterial infection (52). A previous study showed that E2F1 is essential for ISC proliferation (14). ISCs normally express the *E2f1-RE* mRNA isoform, which is transcribed from the same promoter as *E2f1-RA* but lacks an ~800 nt exon that includes the entire Δ(414-828) region found in *E2f1-RA*, resulting in a shorter 5′UTR with 2 uORFs (Fig. 1*D*). The shorter *E2f1-RE* 5′UTR also results in a longer first uORF, as a result of a stop codon that differs from the initial uORF found in *E2f1-RA*. To identify regulatory sequences in the 5′UTR of *E2f1*, we used our existing *E2f1* transgenes (Fig. 3*A* and *SI Appendix*, Fig. S4*C*) to assess mechanisms of 5′UTR regulation that modulate *E2f1* translation levels. Each of the GFP translational sensors was expressed from a temperature sensitive *esgargot* (*esg*)-Gal4 driver (*esg-Gal4^{ts} UAS-GFP*), limiting expression to ISCs and postmitotic progenitors called EBs. The 4 to 5-d-old female flies were shifted to 29 °C for 8, 16, and 24 h to induce expression of GFP before guts were dissected and cells dissociated and run through a Cytoflex flow cytometer. We measured GFP mRNA levels from guts expressing the translational sensors for 24 h, normalized to *Gal4* transcript levels, to monitor changes in mRNA stability conferred by the different UTR variants. Most

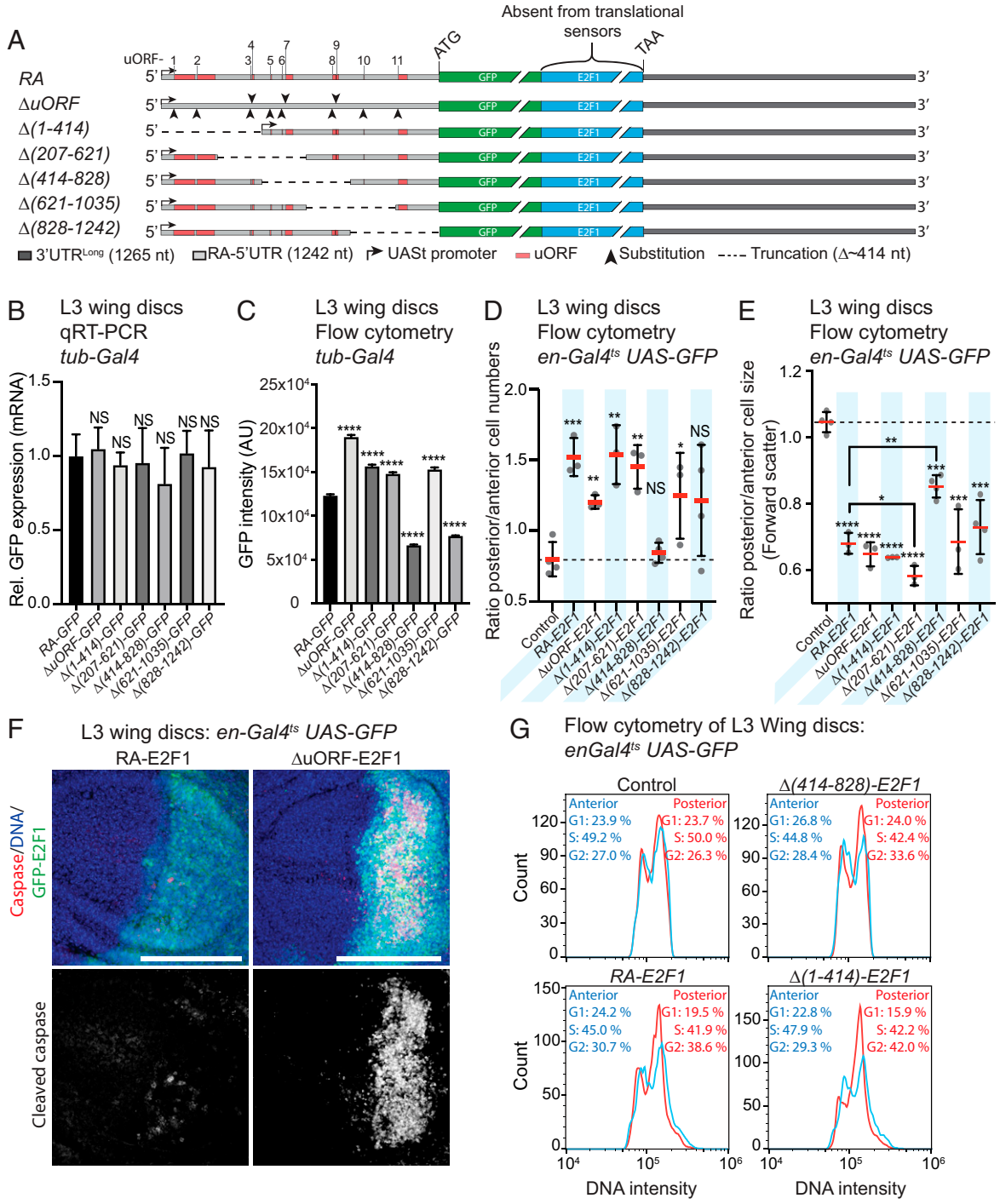

Fig. 3. *E2f1-RA* translation is affected by the 5′UTR sequence. (*A*) Overview of *E2f1* transgenes. (*B*) qRT-PCR analysis of *E2f1* translational sensors expressed in *Drosophila* WDs display similar levels of transcription. (*C*) Accumulations of *E2f1* translational sensors assayed by GFP signal recorded by flow cytometry. (*D*) Comparison of cell numbers in posterior versus anterior WDs expressing *GFP-E2F1* transgenes, quantified by flow cytometry. Data points represent average numbers of individual replicate samples. A cross with *en-Gal4^{ts} UAS-GFP* driver stock and *w^{1118}* flies served as control in *D* and *E*. (*E*) Comparison of cell size in posterior versus anterior WDs expressing *GFP-E2F1* transgenes, assayed by forward scatter using flow cytometry. Data points represent average numbers of individual replicate samples. (*F*) Confocal microscopy Z-projections of L3 wandering larvae. Apoptotic cells were stained using anti-cleaved caspase antibody. (Scale bar: 100 μm.) (*G*) DNA profiles of posterior and anterior WD cells of L3 larvae expressing *GFP-E2F1* transgenes in posterior compartment. Cell cycle phases were estimated in FlowJo using the Watson model. Error bars in *B*, *D*, and *E* represent mean and SD. Error bars in *C* represent median and 95% CI. Student's *t* test performed in *B*–*E* (*$P > 0.05$, **$P > 0.01$,***$P > 0.001$, ****$P > 0.0001$).

transcripts displayed similar levels of expression (Fig. 5*A*). The one exception was the Δ*(414-828)-GFP* transcript, which was expressed at ∼1/3 the level of the *RA-GFP* transcript. ISCs and EBs were identified by RFP expressed from a coexpressed UAS promoter, which allowed gating of RFP+ cells followed by quantification of GFP signal using FlowJo (*SI Appendix*, Fig. S5*B* and Fig. 5 *B* and *C*). We observed increased GFP levels from the Δ*uORF*-, Δ*(1-414)*-, and Δ*(207-621)-GFP* sensors, with the

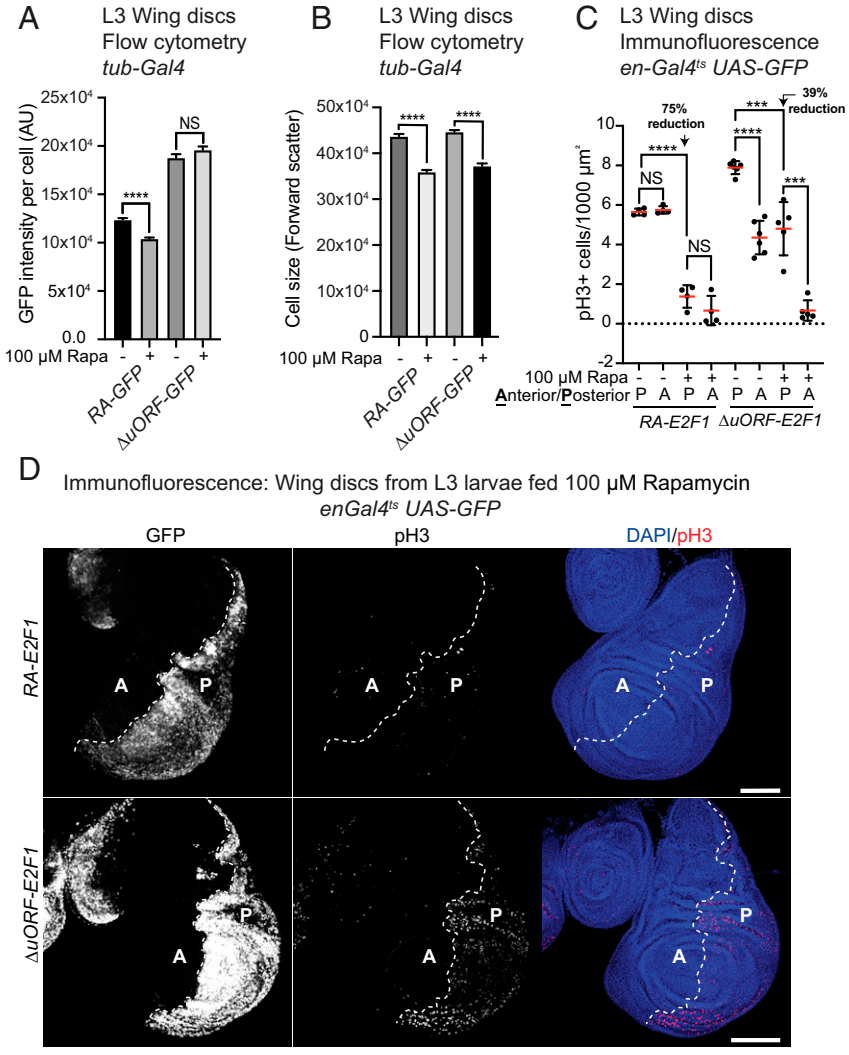

Fig. 4. 5′UTR uORFs render translation and E2F1-dependent proliferation sensitive to TOR. (*A*) Accumulations of *E2f1* translational sensors assayed by GFP signal recorded by flow cytometry, comparing animals fed 100 µM rapamycin (+) with DMSO control (−). (*B*) Comparison of cell size in WDs expressing *GFP-E2F1* transgenes and fed either 100 µM rapamycin (+) or DMSO (−), assayed by forward scatter using flow cytometry. (*C*) Comparison of mitotic cells, assayed by pH3+ cells per 1,000 µm^2, in posterior (P) and anterior (A) WDs from L3 larvae fed either 100 µM rapamycin 4 d after egg laying (AEL) (+) or DMSO 5 d AEL (−) for 20 h. The different timing of rapamycin and DMSO feeding was done to ensure similar WD sizes for comparison. Error bars in *A* and *B* represent median and 95% CI. Error bars in *C* represent mean and SD. Student's *t* test performed in *A*–*C* (*$P >$ 0.05, **$P >$ 0.01,***$P >$ 0.001, ****$P >$ 0.0001). (*D*) Immunostaining of WDs from L3 wandering larvae, fed 100 µM rapamycin, expressing E2F1. (Scale bars in *D* = 100 µm.)

ΔuORF giving the strongest expression (Fig. 5*B*). This is consistent with our observations in WDs. GFP expression from the Δ*(414-828)-GFP* sensor was extremely low; even when normalized to its lower mRNA levels, GFP protein was virtually undetectable in vivo from this transgene (Fig. 5*C*). As we could detect low GFP levels by flow cytometry in WDs, using this transgene, we can rule out that the introduced GFP is defective in this transgene (Fig. 3*C*). In agreement with our results from WDs (Fig. 3 *B*–*E*), this suggests that the 414–828 region of the *E2f1-RA* 5′UTR also positively regulates *E2f1* translation in ISCs. To test whether the regulation of *E2f1* translation through its 5′UTR limits the proliferation of ISCs, the functional E2F1-encoding transgenes were expressed in ISCs (*SI Appendix*, Figs. S4*B* and S8) for 24 h, as described previously. As expected, expression of *RA-E2F1* increased the number of mitotic, pH3+ cells (Fig. 5*D*). This is consistent with previous reports showing that overexpressed E2F1 is sufficient to accelerate mitotic cell cycle progression in *Drosophila* wing and eye discs (Fig. 4) (27, 53, 54) and endocycling in salivary glands and gut enterocytes (13, 14). However, this is an instance of *Drosophila* E2F1 triggering the proliferation of *Drosophila* cells that are essentially quiescent. Expression of Δ*uORF-E2F1* increased ISC proliferation significantly more than *RA-E2F1* (Fig. 5*D*). The levels of *E2f1* mRNA from our various transgenes were similar (*SI Appendix*, Fig. S9), implying that changes in mitotic indices were due mostly to posttranscriptional effects. Deletions within the 5′UTR also had a positive effect on ISC proliferation, with the exception of the Δ(414-828) deletion. Overexpressed Δ*(414-828)-E2F1* had no impact on ISC proliferation, suggesting that sequences in the region 414-828 are essential for translation. Consistently, accumulation of GFP from the translational sensor with the Δ(414-828) 5′UTR was minimal in ISCs (Fig. 5*C*). To further test the importance of the 414–828 region, we constructed a hybrid transgene that lacked the 414-828 region but also had mutations that inactivated the six remaining uORFs [Δ*uORF*Δ*(414-828)-GFP-E2F1*] (*SI Appendix*, Fig. S4*B*). When this Δ*uORF-*Δ*(414-828)-GFP-E2F1* transgene was expressed in ISCs as described previously, we observed proliferation rates that matched those conferred by the ΔuORF transgene, suggesting that the (414-828) region is not required in the absence of uORFs (Fig. 6*A*). This result suggests that sequences in the (414-828) region facilitate translation past uORFs.

Stress Overrides Inhibitory Elements in the *E2f1* mRNA. We next asked how inhibitory and activating *E2f1* mRNA elements affect ISC proliferation during a stress response induced by *Pseudomonas entomophila* (*P.e.*) infection. This stress response includes the activation of EGFR/Ras/Raf and Upd/Jak/Stat signaling, which trigger rapid ISC proliferation (52, 55, 56). We observed increased proliferation in response to *P.e.* in both control and *RA-E2f1* samples, with *RA-E2f1* samples showing a stronger response roughly (52, 55, 56) proportional to their higher rates

of basal ISC proliferation (Fig. 6*B*). In contrast, midguts expressing Δ*uORF-GFP-E2F1* displayed very high rates of mitosis but minimal additional response to *P.e.*, indicating that removal of the uORFs is sufficient to de-repress E2F1 activity to a similar degree as *P.e.* infection (Fig. 6*B*). Further, we observed that the Δ*(414-828)-E2F1* transgene, which failed to show expression or activity in nonstressed flies (Fig. 6*B*), was quite active and expressed quite strongly upon *P.e.* infection (Fig. 6 *B–D*). This suggests that the translational activator site that is deleted in the Δ*(414-828)-E2F1* transgene is not essential for *E2f1* translation during infection stress. The Δ*(414-828)-E2F1* transgene induced somewhat lower levels of proliferation as compared to the *RA-E2F1* transgene (Fig. 6*B*), however, suggesting the 414–828 region still contributes to proliferation upon stress.

***E2f1* Translation Is Increased by Enteric Infection Stress.** Our previous work demonstrated that *E2f1* is posttranscriptionally up-regulated by MAPK signaling, which is activated upon stress in the midgut to increase ISC proliferation (14). Hence, we tested whether MAPK signaling is required to induce *E2f1* expression in the absence of uORFs. We induced expression of *E2f1* transgenes (*RA-E2F1*, Δ*uORF-E2F1*) (*SI Appendix*, Fig. S4*B*) or translational sensors (*RA-GFP*, Δ*uORF-GFP*) (*SI Appendix*, Fig. S4*C*), together with MEK^{RNAi}, for 3 d and quantified proliferation and translation of GFP, respectively. In addition, we treated one set of these flies with *P.e*. for 20 h, leaving a second set as controls. We observed increased accumulation of GFP when infecting flies expressing RA-GFP (Fig. 6*E*), consistent with increased proliferation (Fig. 6*F*). This demonstrates that *E2f1* translation rate increases specifically in ISCs upon stress. Similar to RA-GFP, translation of the ΔuORF-GFP sensor also increased during *P.e.* infection, but proliferation was already high and did not increase. These observations suggest that while stress can induce *E2f1* translation independently of the uORFs, the removal of the uORFs probably saturates *E2f1* expression to a level that drives maximal proliferation. When coexpressing MEK^{RNAi} with *RA-GFP* or *RA-E2F1* in ISCs, we observed significantly decreased levels of GFP or proliferation (Fig. 6 *E* and *F*), consistent with previous reports that show that EGFR signaling is required for ISC proliferation (14). This is similar to what we observed with Δ*uORF-GFP* and Δ*uORF-E2F1*, namely that both translation and proliferation were sensitive to MEK activity. When combining MEK^{RNAi} with *P.e.* infection, both proliferation and translation were reduced in cells expressing *RA-E2F1* or *RA-GFP*, respectively (Fig. 6 *E* and *F*). This was also the case when expressing Δ*uORF-GFP* or Δ*uORF-E2F1*. In conclusion, we have demonstrated that translation of *E2f1* increases in response to *P.e.* infection in an MEK-dependent manner. We have also demonstrated that stress, induced by enteric infection, and MEK activity promote *E2f1* translation through a mechanism independent of the uORFs.

Discussion

***E2f1* mRNA Acts as a Growth Sensor in Mitotically Proliferating Cells.** Previous studies have shown that *E2f1* expression is posttranscriptionally regulated by growth signaling, including EGFR and TOR signaling, and that this regulatory mechanism controls endocycles in polyploid cells (13, 14). Here, we demonstrate that increasing the translation of *E2f1* mRNA by removing its 5′UTR uORFs can also accelerate mitotic cell cycles. Our data support a model (Fig. 7) wherein *E2f1* mRNA acts as a translationally regulated growth sensor that regulates proliferation in *Drosophila* wing disc cells and ISCs. This mechanism is analogous to what has been described for regulation of the budding and fission yeast cell cycles, which are limited by translational regulation of Cln3 (2) and cdc25 (4), respectively. TOR and EGFR signaling are well-known regulators of both cell growth and protein translation (57–59), so our observation that these pathways also stimulate *E2f1* translation reveals a regulatory link that couples the growth rate of a cell to its proliferation rate. This translational mechanism is noteworthy because it provides an alternative to the prevailing transcriptional model for growth signaling control of the animal cell cycle. Whereas the transcriptional model is supported by extensive data, it is unlikely to account for all aspects of growth-dependent cell cycle control because its transcription-dependent effectors, Cyclins D1 to D3, are nonessential genes, and growth factors and nutrients can stimulate cell cycle progression even without them (10–12).

Although E2F1 may be the predominant translationally regulated growth sensor in most *Drosophila* cells, other cell cycle regulators may also be regulated by similar mechanisms in animal cells. Previous reports have indicated that Cyclin E1 and Cyclin D1 are translationally regulated in mammals (60–64), suggesting that multiple cell cycle regulators could serve as growth sensors. We show here that translational regulation of *E2f1* is strongly mediated by sequences in its 5′UTR, implying that the expression of mRNA isoforms with different 5′ UTRs can be decisive in tissue specific responses to upstream regulation. In turn, this implies that the specific set of cell cycle regulators that serve as growth sensors may differ by cell and tissue type and in different organisms.

***E2f1* Translation in Imaginal Discs.** Our study suggests that the *E2f1-RA* mRNA isoform possesses a TOR-responsive element in its 5′UTR (Fig. 2). Further, our results demonstrate that efficient *E2f1* translation is less dependent on TOR activity in the absence of uORFs (Fig. 4). TOR-dependent translation through uORFs has so far not been widely studied; however, a previous study in *Arabidopsis* reported that ribosome reinitiation following uORFs could be affected by TOR (65). Another study using mammalian cells showed that a uORF is required for the expression of a truncated isoform of C/EBP, through an unknown mechanism dependent on TOR activity (66). Among the TOR-responsive *E2f1* isoforms, the *E2f1-RA* and *E2f1-RD* isoforms have the most uORFs (11 and 9, respectively). It is tempting to assume that the additive effect of multiple uORFs is responsible for TOR-dependent *E2f1* translation; however, we cannot exclude that a specific subset of uORFs are more potent translation attenuators. In fact, uORF-mediated translation attenuation depends in part on the associated Kozak element and uORF length (20, 41). With our truncated translational sensors that lack the first 7 uORFs (Fig. 3), Δ(1-414)- and Δ(207-621)-GFP, we observed consistent increases in translation both in WD cells and ISCs. However, these de-repression effects were less than we observed with the ΔuORF-GFP sensor. We infer that among the first seven uORFs, at least two uORFs dampen *E2f1* expression, assuming there are no other regulatory motifs involved. Due to the possibility of unknown regulatory elements in the *E2f1* 5′UTR, pinpointing which uORFs attenuate translation would require individual and combined removal of uORFs. Further studies will be necessary to determine which uORFs are translated in vivo and how they affect *E2f1* translation in different cell types and under different growth conditions. Moreover, we have not taken mRNA secondary structure into consideration, and we cannot exclude the possibility that our ΔuORF transgenes have introduced changes in RNA secondary structure or other unforeseen effects on *E2f1* translation.

We also identified a region, between positions 414-828 of the *E2f1-RA* 5′UTR, that is required for efficient *E2f1* translation in wing disc and midgut cells. This region only exists in the *E2f1-RA* and *-RD* isoforms, which are the two *E2f1* isoforms most highly expressed in the wing disc (Fig. 1). *E2f1-RA* and *-RD* are also two of the three isoforms predicted to be TOR-sensitive (Fig. 2), suggesting the 414-828 region serves as a potential regulatory site for TOR. Surprisingly, the expression of the transgenes with truncations that flank

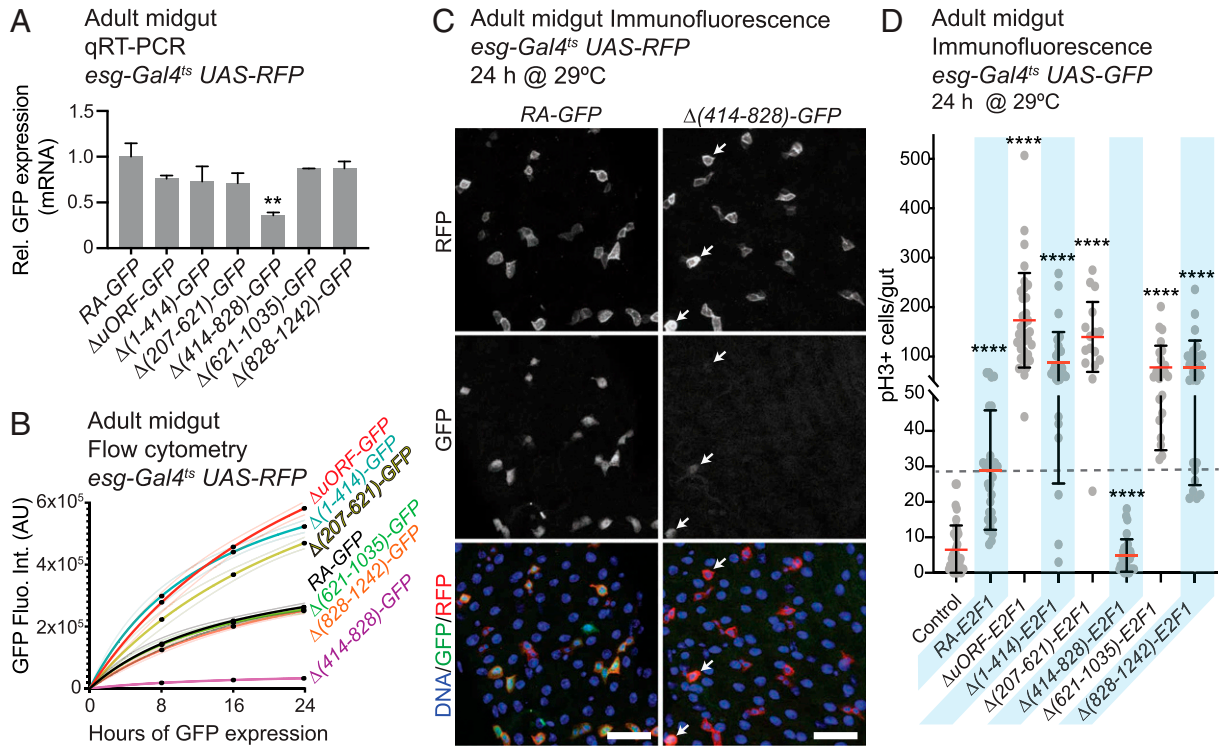

Fig. 5. 5′UTRs affect E2F1-dependent proliferation in the midgut. (*A*) qRT-PCR analysis of *E2f1* translational sensors expressed in *Drosophila* midgut display similar levels of transcription, with the exception of Δ(414-828)-GFP. Temperature sensitive expression controlled by *esgGal4^{ts} UAS-RFP*. The 24 h expression was induced by 29 °C temperature shift. (*B*) Accumulations of *E2f1* translational sensors assayed by GFP signal recorded by flow cytometry 8, 16, and 24 h post induction. Expression was induced by 29 °C temperature shift. ISCs were sorted by Hoechst and RFP. (*C*) Confocal images of adult midguts expressing translational sensors. Only weak GFP signal can be detected in guts expressing *Δ(414-828)-GFP* (marked with arrows). (*D*) *E2f1* transgenes expressed in *Drosophila* midgut ISCs, using *esgGal4^{ts} UAS-GFP* driver. The 3 to 4 d old females were shifted to 29 °C for 24 h, and proliferation was assayed by counting the total number of pH3+ cells per midgut. A cross with *esg-Gal4^{ts} UAS-GFP* driver stock and *W^{1118}* flies served as control. Student's *t* test performed in *A* and *D* (*$P > 0.05$, **$P > 0.01$,***$P > 0.001$, ****$P > 0.0001$). (Scale bar in *C* = 30 μm.)

and overlap the 414-828 region [Δ(207-621) and Δ(621-1035)] did not display similar effects on translation as the Δ(414-828) transgene. This suggests that regulatory sequence(s) within the 414-621 region and 621-828 region redundantly enhance *E2f1* expression in wing discs. There are two regions around the sixth–seventh uORFs and eighth–ninth uORFs conserved among several species of *Drosophila* (*SI Appendix*, Fig. S3) that lie on opposite sides of the 414-828 region. These may be translational enhancer sites. In addition, we used RBPsuite (67) to predict potential protein binding sites that may be involved in translational regulation. Interestingly, there are predicted binding sites for several eukaryotic initiation factors (eIFs) near the conserved eighth and ninth uORFs in addition to the site near the E2F1 start codon (*SI Appendix*, Fig. S10). How eIFs might contribute to enhanced translation in wing discs (33) without serving an IRES (*SI Appendix*, Fig. S7) remains obscure but may be an interesting possibility to investigate.

***E2f1* Translation in ISCs.** ISCs predominantly express the *E2f1-RE* mRNA isoform, which lacks the exon containing the entire 414-828 region found in the *E2f1-RA* isoform. Based on our data, this suggests that E2F1 protein expression should be low in ISCs. However, the *E2f1-RE* isoform also possesses fewer uORFs than the *E2f1-RA* isoform (2 vs. 11, respectively), and this could compensate for the lack of translational enhancement by the 414-828 region. In fact our results show that in ISCs, the 414-828 region is dispensable in the absence of uORFs (Fig. 6*A*). This suggests that *E2f1-RE* translation is less dependent of input from TOR. The expression of *E2f1-RE* in ISCs, instead of *E2f1-RA*, may thus reflect an adaption to respond to EGFR signaling rather than to TOR signaling (14). ISCs encounter situations where cells need to proliferate in response to tissue damage rather than growth. Although ISCs require TOR for growth in basal conditions, this requirement can be bypassed by EGFR/MAPK signaling during episodes of stress-induced ISC activation (14). Furthermore, enforced TOR activity is not sufficient to activate ISC proliferation (28, 68–70). Here, we have shown that *E2f1* translation in ISCs is also enhanced in response to infection-induced stress (Fig. 6*B*), which activates EGFR signaling. Interestingly, we found that the ΔuORF-GFP translational sensor is sensitive to MEK^{RNAi} (Fig. 6 *E* and *F*), suggesting that MEK/MAPK signaling can regulate *E2f1* translation independently of the uORFs. Evidently, the *E2f1* mRNA can respond translationally to multiple different proliferation signals through distinct mechanisms. Our data suggest that the different *E2f1* mRNA isoforms provide different mechanisms for controlling *E2f1* translation in response to different inputs, in a cell type–specific manner. Identifying the transacting factors that mediate the effects of MAPK, TOR, and other signaling pathways on *E2f1* translation should further illuminate how growth signaling interfaces with cell cycle control. It is likely that MAPK, TOR, and other growth signaling pathways regulate translation of other critical cell cycle regulators beyond E2F1, and that the mechanisms illuminated here may come into play in many if not most animal cells.

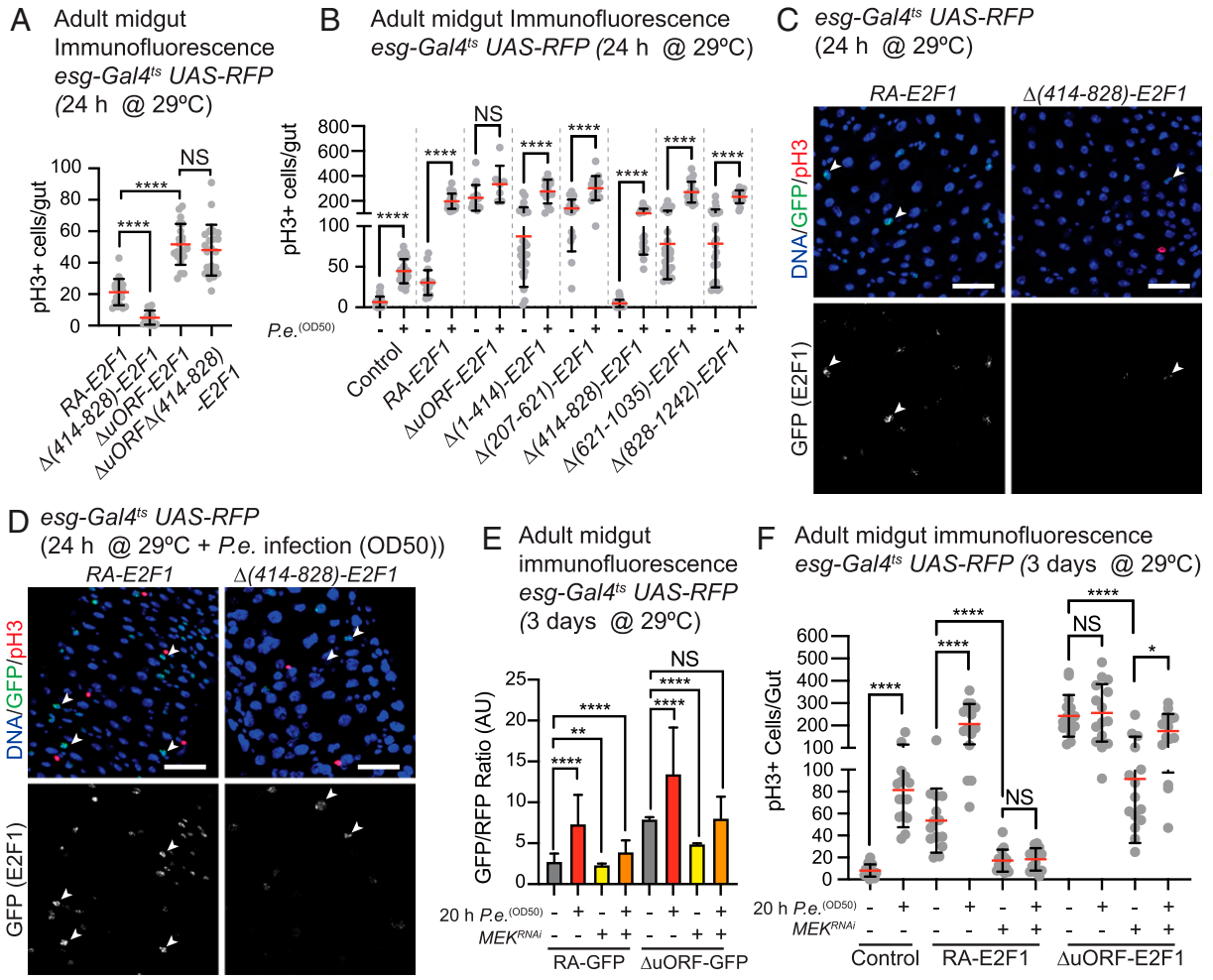

Fig. 6. *P.e.* infection of adult midguts expressing *E2f1* transgenes. (*A* and *B*) *E2f1* transgenes expressed in *Drosophila* midgut ISCs, using *esgGal4*^{ts} *UAS-RFP* driver. The 4 to 5 d old females were shifted to 29 °C for 24 h, and proliferation was assayed by counting total number of pH3+ cells per midgut. The flies in *B* were fed either 5% sucrose (−) or 5% sucrose + *P.e.* (OD50) (+). A cross with *esg-Gal4*^{ts} *UAS-RFP* driver stock and W^{1118} flies served as control in *B* and *E*. (*C* and *D*) Confocal images of samples from *B*. Examples of GFP positive cells marked by arrowheads. (*E*) GFP translational sensors coexpressed, with or without MEK^{RNAi}, in *Drosophila* midgut ISCs as in *D*. GFP intensity of individual cells measured by flow cytometry. (*F*) *E2f1* transgenes coexpressed, with (+) or without (−) MEK^{RNAi}, in *Drosophila* midgut ISCs, using *esgGal4*^{ts} *UAS-RFP* driver. The 3 to 4 d old females were shifted to 29 °C for 24 h while being fed OD50 *P.e.* (+) or sucrose (−), and proliferation was assayed by counting total number of pH3+ cells per midgut. Error bars in *A* and *D* represent mean and SD. Error bars in *E* represent median and 95% CI. Student's *t* test performed in *A*, *D*, and *E* (*$P > 0.05$, **$P > 0.01$,***$P > 0.001$, ****$P > 0.0001$). (Scale bars in *B* and *C* = 30 μm.)

Methods and Materials

Immunostaining. After dissection, samples were fixed in phosphate buffered saline (PBS) with 4% paraformaldehyde for 30 min at room temperature, washed in PBS with 0.015% Triton X-100, and blocked in PBS with 0.15% Triton X-100 and 10% normal goat serum (NGS) for at least 1 h at room temperature. WDs and adult midgut samples were then stained with primary antibodies at 4 °C overnight with the following dilutions: guinea pig **α-E2F1** (X. Bi, Dalian Medical University, 1:200), rabbit **α-Cleaved Caspase-3** (Cell Signaling, 1:100), and rabbit **α-PH3** (Millipore, 1:1,000). DAPI (Thermo Fisher Scientific, 1:1,000) was used to label nuclei. Eye discs were stained with affinity purified rabbit **α-E2F1** (N. Dyson, Harvard Medical School, 1:100). Staining was detected by Alexa Fluor 488, 568, or 633 conjugated species appropriate secondary antibodies (Thermo Fisher Scientific, 1:1,000). Images were taken on a Leica SP8 confocal microscope at the Cell Imaging and Analysis Network, McGill University, and a Leica SP8 confocal microscope at the Cell Imaging Core at the University ofUtah. For quantification of endogenous E2f1 expression and pH3+ cells from immunohistochemistry samples, see details in *SI Appendix, Supplementary Materials and Methods*.

Complementary DNA Synthesis and qRT-PCR on *Drosophila* Tissue. Adult midguts and larval tissues were dissected in PBS and transferred to PBS on ice. PBS was then replaced with lysis buffer from Ambion RNAqueous kit, and samples were vortexed and supplemented with EtOH before being stored at −80 °C. Samples were stored no longer than 1 wk before RNA extraction. RNA from lysate was purified using the Ambion RNAqueous micro kit following the manufacturer's recommended protocol. Total RNA (~300 ng) was reverse transcribed using Invitrogen SuperScript III reverse transcriptase (Thermo Fisher Scientific) with oligo-dT primers (DNA/Peptide Facility, Health Sciences Center Cores at the University of Utah). qRT-PCR reactions of 10 μL total volume were assembled using complementary DNA (cDNA) equivalent to 0.15 ng total RNA, 500 nM gene specific forward and reverse primers, and 5 μL iTAQ Universal SYBR Green Supermix (Bio-Rad). qRT-PCR reactions were run on a C1000 thermal cycler with a CFX-384 module (Bio-Rad). Samples were run as three technical and three biological replicates. Relative expression levels were normalized to Gal4 mRNA expression. Primers recognizing GFP transcripts were used to measure transgene expression. For quantification of endogenous E2F1 and ectopically expressed Rheb levels in WD, we normalized to *Drosophila* DP transcription factor (dDP). Statistical significance of mRNA expression was assessed in Prism 8 by Student's *t* test (*$P < 0.05$, **$P < 0.01$, ***$P < 0.001$, ****$P < 0.0001$). Primers used are listed in *SI Appendix*, Table S2.

cDNA Synthesis and qRT-PCR on *Drosophila* S2R+ Cells. See *SI Appendix, Supplementary Materials and Methods*.

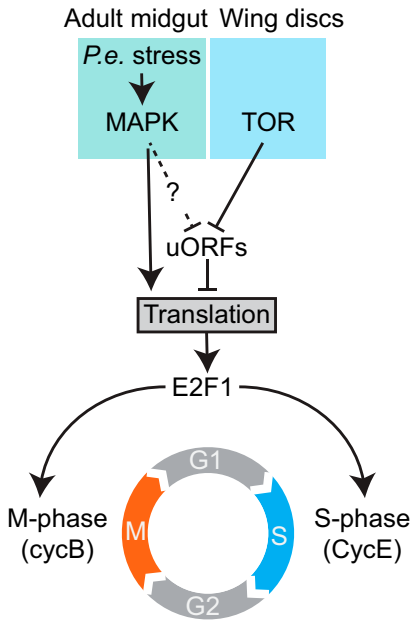

Fig. 7. Cell cycle control by *E2f1* translation. Proposed model of E2F1 dependent cell cycle regulation. In ISCs, *P.e.*-induced stress enhances *E2f1* translation through MAPK signaling, which in turn accelerates proliferation. In WDs, *E2f1* translation is suppressed by multiple uORFs in the *E2f1* 5′UTR. *E2f1* translation is relieved by TOR activity.

Real Time Measurement of Translational Sensors in S2R+ Cells. See *SI Appendix, Supplementary Materials and Methods*.

***E2f1* Isoforms Abundance Estimation via Cufflinks.** For the analysis of adult midgut cells, raw reads from the SRP047054 entry (71) on the NCBI Sequence Read Archive (SRA) were downloaded using the SRA Toolkit version 2.9.2. Raw reads were aligned to the *Drosophila* genome version 6 using TopHat2 version 2.0.9 (72), and Bowtie2 version 2.1.0. *E2f1* isoform abundance was estimated using Cufflinks version 2.2.1 (73). The *E2f1* entry in the *Drosophila* genome annotation file used in conjunction with Cufflinks was modified as follows (*SI Appendix*): the 3′UTR of isoforms FBtr0334678, FBtr0084117, and FBtr0084119 were altered to match that of the other *E2f1* isoforms; the exon at coordinates 3R: 21624245–21624292 was removed from isoforms FBtr0345217 and FBtr0334678. These modifications resulted in the difference between transcripts being entirely in their 5′UTR region.

Fly Stocks. Fly stocks used in this paper are summarized in *SI Appendix*, Table S1, listed by the order they appear. Crosses containing $Gal80^{ts}$ were maintained at 18 °C until shifted to 29 °C at the desired timepoint. Other crosses were raised at 25 °C. *Tsc1*$^{-}$ ($Tsc1^{Q87X}$), $E2F1^{RS5}$ and $Tsc1^{Q87X}$, $E2F1^{\Delta RA}$ were generated by meiotic recombination. An unrelated homozygous lethal mutation in $E2F1^{\Delta RA}$ was recombined out. Transgenic lines were established through PhiC31 integrase-mediated transformation (Best Gene). UASTattB vectors, carrying inserted transgenes, were used to transform BDSC stock # 9744 (PBac{yellow[+]-attP-9A}VK00027), guiding insertion of transgene into the 89E11 cytosite.

Rapamycin Feeding Larvae. Water was mixed in with complete fly food until fluid enough to pipette with a 25 mL pipette. Rapamycin in DMSO was added to fly food to a final concentration of 100 μM. An equal amount, 1:1,000, DMSO was added to control. Fly food was then thoroughly mixed by vortexing. Then, 5 mL fly food was pipetted on 60 × 15 mm polystyrene Petri dishes with ventilation ribs (Sigma Aldrich). Larvae were transferred to Petri dishes 20 to 24 h prior to dissection and incubated at 29 °C.

Construct Generation. See *SI Appendix, Supplementary Materials and Methods*.

DNA Profiling and Measurement of GFP Translational Sensors Expressed in WDs by Flow Cytometry. WDs from L3 larvae were dissected and washed in PBS and transferred in ∼10 μL PBS to 1.5 mL Eppendorf tubes on ice. Then, 150 μL 10× trypsin (Thermo Fisher Scientific) was added to discs before incubation at room temperature on an Eppendorf shaker (600 rpm) for 2 h. Hoechst was added after 1 h to a final concentration of 5 μg/mL. Trypsin was inactivated by adding fetal bovine serum to a final concentration of 2%. Samples were briefly vortexed and filtered through a 20 μm cell strainer. Samples were protected from light until run through Beckman Coulter Cytoflex LX. Data were analyzed using FlowJo and gated as in *SI Appendix*, Fig. S5*A*. For representation of GFP levels, data points from final gate (fourth) were extracted and plotted in Prism 8. For comparison of posterior and anterior cells in *en-Gal4*^{ts} *UAS-GFP* wing discs, the posterior cell population (GFP+) was defined by presence of GFP (fourth gate), whereas anterior cell population (GFP−) was defined by absence of GFP (third gate - fourth gate). Ratio metric comparison of cell numbers was done by dividing the number of GFP+ cells with GFP− cells. Ratio metric comparison of cell size was done by dividing average forward scatter of GFP+ cells with GFP− cells. For DNA profiling, posterior and anterior cells were analyzed in FlowJo using the Watson cell cycle algorithm. Statistical significance of GFP expression was assessed in Prism 8 by Student's *t* test (*$P < 0.05$, **$P < 0.01$, ***$P < 0.001$, ****$P < 0.0001$).

Measurement of GFP Translational Sensors Expressed in Adult Midgut by Flow Cytometry. Midguts from adult flies were dissected in Schneider's medium and transferred to Schneider's medium on ice, where they were stored until completion of dissection. Collagenase was added to a final concentration of 0.2 U/mL and incubated for 1 h at 29 °C with shaking (850 rpm). Cells were harvested by centrifugation 2,500 rpm for 12 min and were resuspended in 500 μL 1× PBS with 40 μM Hoechst. Cells were passed through a 70 μm cell strainer before samples were measured on a Beckman Coulter Cytoflex LX. Data were analyzed using FlowJo. Singlet cells were first gated by FSC-A and FSC-Width, and then cells stained with Hoechst were gated as in *SI Appendix*, Fig. S5*B*. ISCs and EBs were then gated by RFP expressed under esgGal4, UAS-RFP. Cells of similar size were then gated and measured for GFP expression. For representation of GFP levels, data points from final gate were extracted and plotted in Prism 8. Statistical significance of GFP expression was assessed in Prism 8 by Student's *t* test (*$P < 0.05$, **$P < 0.01$, ***$P < 0.001$, ****$P < 0.0001$).

***P.e.* Infection.** The 4 to 5-d-old flies were starved for 2 h prior to infection in vials containing an acetate cellulose vial plug soaked in 8 mL 5% sucrose to prevent desiccation. Flies were treated for 20 h with either 1 mL 5% sucrose or 1 mL *P.e.* (optical density [OD] = 50), from a 20 to 24 h culture grown at 29 °C, 200 rpm in Luria broth containing 100 μg rifampicin, resuspended in 5% sucrose. *P.e.* and control solutions were distributed on ∼6 × 6 cm Whatman paper.

Clone Generation in Eye Discs. See *SI Appendix, Supplementary Materials and Methods*.

Protein Extraction and Western Blot. See *SI Appendix, Supplementary Materials and Methods*.

Data Availability. All study data are included in the article and/or *SI Appendix*.

ACKNOWLEDGMENTS We thank X. Bi and N. Dyson for antibodies and the University of Utah's Flow Cytometry and Cell Imaging shared resources. The work was supported by the Huntsman Cancer Foundation, European Research Council (ERC) Advanced Grant 268515 (to B.A.E.), NIH R01 GM126033 (to B.A.E.), and a grant from the Natural Science and Engineering Research Council of Canada RGPIN-2019-05699 (to N.-S.M).

1. K. M. Schmoller, J. J. Turner, M. Kõivomägi, J. M. Skotheim, Dilution of the cell cycle inhibitor Whi5 controls budding-yeast cell size. *Nature* **526**, 268–272 (2015).
2. M. Polymenis, E. V. Schmidt, Coupling of cell division to cell growth by translational control of the G1 cyclin CLN3 in yeast. *Genes Dev.* **11**, 2522–2531 (1997).
3. M. B. Ginzberg *et al.*, Cell size sensing in animal cells coordinates anabolic growth rates and cell cycle progression to maintain cell size uniformity. *eLife* **7**, e26957 (2018).
4. R. R. Daga, J. Jimenez, Translational control of the cdc25 cell cycle phosphatase: A molecular mechanism coupling mitosis to cell growth. *J. Cell Sci.* **112**, 3137–3146 (1999).
5. M. B. Ginzberg, R. Kafri, M. Kirschner, Cell biology. On being the right (cell) size. *Science* **348**, 1245075 (2015).
6. E. Zatulovskiy, J. M. Skotheim, On the molecular mechanisms regulating animal cell size homeostasis. *Trends Genet.* **36**, 360–372 (2020).
7. R. A. Weinberg, Chapter 8: pRb and Control of the Cell Cycle Clock in *The Biology of Cancer* (Garland Science, Taylor and Francis Group, ed. 2, New York, 2014), pp. 394–305.
8. B. Alberts, Chapter 17: The Cell Cycle in *Molecular Biology of the Cell* (Garland Science, Taylor and Francis Group, ed. 6, New York, 2015), pp. 1012–1013.

9. H. F. Lodish, *Molecular Cell Biology* (W. H. Freeman and Co., ed. 9, New York, 2020), 867–875.
10. C. A. Meyer *et al.*, Drosophila Cdk4 is required for normal growth and is dispensable for cell cycle progression. *EMBO J.* **19**, 4533–4542 (2000).
11. M. Malumbres *et al.*, Mammalian cells cycle without the D-type cyclin-dependent kinases Cdk4 and Cdk6. *Cell* **118**, 493–504 (2004).
12. K. Kozar *et al.*, Mouse development and cell proliferation in the absence of D-cyclins. *Cell* **118**, 477–491 (2004).
13. N. Zielke *et al.*, Control of Drosophila endocycles by E2F and CRL4(CDT2). *Nature* **480**, 123–127 (2011).
14. J. Xiang *et al.*, EGFR-dependent TOR-independent endocycles support Drosophila gut epithelial regeneration. *Nat. Commun.* **8**, 15125 (2017).
15. X. Wang, C. G. Proud, Nutrient control of TORC1, a cell-cycle regulator. *Trends Cell Biol.* **19**, 260–267 (2009).
16. G. J. Brunn *et al.*, Phosphorylation of the translational repressor PHAS-I by the mammalian target of rapamycin. *Science* **277**, 99–101 (1997).
17. W. J. Faller *et al.*, Mtorc1 mediated translational elongation is limiting for intestinal tumour initiation and growth. *Gut* **63**, A130–A131 (2014).
18. A. C. Gingras, S. G. Kennedy, M. A. O'Leary, N. Sonenberg, N. Hay, 4E-BP1, a repressor of mRNA translation, is phosphorylated and inactivated by the Akt(PKB) signaling pathway. *Genes Dev.* **12**, 502–513 (1998).
19. P. D. Lu, H. P. Harding, D. Ron, Translation reinitiation at alternative open reading frames regulates gene expression in an integrated stress response. *J. Cell Biol.* **167**, 27–33 (2004).
20. S. Schleich *et al.*, DENR-MCT-1 promotes translation re-initiation downstream of uORFs to control tissue growth. *Nature* **512**, 208–212 (2014).
21. S. E. Calvo, D. J. Pagliarini, V. K. Mootha, Upstream open reading frames cause widespread reduction of protein expression and are polymorphic among humans. *Proc. Natl. Acad. Sci. U.S.A.* **106**, 7507–7512 (2009).
22. N. V. Sharkov, G. Ramsay, A. L. Katzen, The DNA replication-related element-binding factor (DREF) is a transcriptional regulator of the Drosophila myb gene. *Gene* **297**, 209–219 (2002).
23. A. C. Hsieh *et al.*, The translational landscape of mTOR signalling steers cancer initiation and metastasis. *Nature* **485**, 55–61 (2012).
24. A. E. Koromilas, A. Lazaris-Karatzas, N. Sonenberg, mRNAs containing extensive secondary structure in their 5′ non-coding region translate efficiently in cells overexpressing initiation factor eIF-4E. *EMBO J.* **11**, 4153–4158 (1992).
25. N. Nandagopal, P. P. Roux, Regulation of global and specific mRNA translation by the mTOR signaling pathway. *Translation (Austin)* **3**, e983402 (2015).
26. T. C. Hsieh, B. N. Nicolay, M. V. Frolov, N. S. Moon, Tuberous sclerosis complex 1 regulates dE2F1 expression during development and cooperates with RBF1 to control proliferation and survival. *PLoS Genet.* **6**, e1001071 (2010).
27. T. P. Neufeld, A. F. de la Cruz, L. A. Johnston, B. A. Edgar, Coordination of growth and cell division in the Drosophila wing. *Cell* **93**, 1183–1193 (1998).
28. L. J. Saucedo *et al.*, Rheb promotes cell growth as a component of the insulin/TOR signalling network. *Nat. Cell Biol.* **5**, 566–571 (2003).
29. F. D. Karim, G. M. Rubin, Ectopic expression of activated Ras1 induces hyperplastic growth and increased cell death in Drosophila imaginal tissues. *Development* **125**, 1–9 (1998).
30. P. Zhang *et al.*, A balance of Yki/Sd activator and E2F1/Sd repressor complexes controls cell survival and affects organ size. *Dev. Cell* **43**, 603–617.e5 (2017).
31. H. Barcelo, M. J. Stewart, Altering Drosophila S6 kinase activity is consistent with a role for S6 kinase in growth. *Genesis* **34**, 83–85 (2002).
32. D. A. Prober, B. A. Edgar, Ras1 promotes cellular growth in the Drosophila wing. *Cell* **100**, 435–446 (2000).
33. K. Leppek, R. Das, M. Barna, Functional 5′ UTR mRNA structures in eukaryotic translation regulation and how to find them. *Nat. Rev. Mol. Cell Biol.* **19**, 158–174 (2018).
34. M. L. Truitt, D. Ruggero, New frontiers in translational control of the cancer genome. *Nat. Rev. Cancer* **16**, 288–304 (2016).
35. A. G. Hinnebusch, I. P. Ivanov, N. Sonenberg, Translational control by 5′-untranslated regions of eukaryotic mRNAs. *Science* **352**, 1413–1416 (2016).
36. P. R. Araujo *et al.*, Before it gets started: Regulating translation at the 5′ UTR. *Comp. Funct. Genomics* **2012**, 475731 (2012).
37. P. F. Renz, F. Valdivia-Francia, A. Sendoel, Some like it translated: Small ORFs in the 5'UTR. *Exp. Cell Res.* **396**, 112229 (2020).
38. S. L. Schuster, A. C. Hsieh, The untranslated regions of mRNAs in cancer. *Trends Cancer* **5**, 245–262 (2019).
39. A. Larkin *et al.*, FlyBase Consortium, FlyBase: Updates to the Drosophila melanogaster knowledge base. *Nucleic Acids Res.* **49** (D1), D899–D907 (2021).
40. M. Kim, J. P. Tang, N. S. Moon, An alternatively spliced form affecting the Marked Box domain of Drosophila E2F1 is required for proper cell cycle regulation. *PLoS Genet.* **14**, e1007204 (2018).
41. S. Schleich, J. M. Acevedo, K. Clemm von Hohenberg, A. A. Teleman, Identification of transcripts with short stuORFs as targets for DENR•MCTS1-dependent translation in human cells. *Sci. Rep.* **7**, 3722 (2017).
42. A. W. van der Velden, H. O. Voorma, A. A. Thomas, Vector design for optimal protein expression. *Biotechniques* **31**, 572, 574, 576–580, passim (2001).
43. K. Han *et al.*, Parallel measurement of dynamic changes in translation rates in single cells. *Nat. Methods* **11**, 86–93 (2014).
44. M. R. Bradley-Gill *et al.*, Alternate transcripts of the Drosophila "activator" E2F are necessary for maintenance of cell cycle exit during development. *Dev. Biol.* **411**, 195–206 (2016).
45. K. G. Golic, M. M. Golic, Engineering the Drosophila genome: Chromosome rearrangements by design. *Genetics* **144**, 1693–1711 (1996).
46. E. Ryder *et al.*, The DrosDel collection: A set of P-element insertions for generating custom chromosomal aberrations in Drosophila melanogaster. *Genetics* **167**, 797–813 (2004).
47. R. Elkon, A. P. Ugalde, R. Agami, Alternative cleavage and polyadenylation: Extent, regulation and function. *Nat. Rev. Genet.* **14**, 496–506 (2013).
48. B. Tian, J. L. Manley, Alternative cleavage and polyadenylation: The long and short of it. *Trends Biochem. Sci.* **38**, 312–320 (2013).
49. S. Shibutani, L. M. Swanhart, R. J. Duronio, Rbf1-independent termination of E2f1-target gene expression during early Drosophila embryogenesis. *Development* **134**, 467–478 (2007).
50. A. H. Brand, N. Perrimon, Targeted gene expression as a means of altering cell fates and generating dominant phenotypes. *Development* **118**, 401–415 (1993).
51. A. G. Hinnebusch, Translational regulation of GCN4 and the general amino acid control of yeast. *Annu. Rev. Microbiol.* **59**, 407–450 (2005).
52. H. Jiang *et al.*, Cytokine/Jak/Stat signaling mediates regeneration and homeostasis in the Drosophila midgut. *Cell* **137**, 1343–1355 (2009).
53. M. Asano, J. R. Nevins, R. P. Wharton, Ectopic E2F expression induces S phase and apoptosis in Drosophila imaginal discs. *Genes Dev.* **10**, 1422–1432 (1996).
54. L. A. Buttitta, A. J. Katzaroff, C. L. Perez, A. de la Cruz, B. A. Edgar, A double-assurance mechanism controls cell cycle exit upon terminal differentiation in Drosophila. *Dev. Cell* **12**, 631–643 (2007).
55. N. Buchon, N. A. Broderick, T. Kuraishi, B. Lemaitre, Drosophila EGFR pathway coordinates stem cell proliferation and gut remodeling following infection. *BMC Biol.* **8**, 152 (2010).
56. H. Jiang, B. A. Edgar, Intestinal stem cells in the adult Drosophila midgut. *Exp. Cell Res.* **317**, 2780–2788 (2011).
57. M. Cargnello, P. P. Roux, Activation and function of the MAPKs and their substrates, the MAPK-activated protein kinases. *Microbiol. Mol. Biol. Rev.* **75**, 50–83 (2011).
58. G. Y. Liu, D. M. Sabatini, mTOR at the nexus of nutrition, growth, ageing and disease. *Nat. Rev. Mol. Cell Biol.* **21**, 183–203 (2020).
59. E. Minnee, W. J. Faller, Translation initiation and its relevance in colorectal cancer. *FEBS J.* **288**, 6635–6651 (2021).
60. C. J. Nelsen, D. G. Rickheim, M. M. Tucker, L. K. Hansen, J. H. Albrecht, Evidence that cyclin D1 mediates both growth and proliferation downstream of TOR in hepatocytes. *J. Biol. Chem.* **278**, 3656–3663 (2003).
61. M. M. Goggin *et al.*, Rapamycin-sensitive induction of eukaryotic initiation factor 4F in regenerating mouse liver. *Hepatology* **40**, 537–544 (2004).
62. L. K. Mullany *et al.*, Akt-mediated liver growth promotes induction of cyclin E through a novel translational mechanism and a p21-mediated cell cycle arrest. *J. Biol. Chem.* **282**, 21244–21252 (2007).
63. M. C. Lai, W. C. Chang, S. Y. Shieh, W. Y. Tarn, DDX3 regulates cell growth through translational control of cyclin E1. *Mol. Cell. Biol.* **30**, 5444–5453 (2010).
64. W. J. Faller *et al.*, mTORC1-mediated translational elongation limits intestinal tumour initiation and growth. *Nature* **517**, 497–500 (2015).
65. M. Schepetilnikov *et al.*, TOR and S6K1 promote translation reinitiation of uORF-containing mRNAs via phosphorylation of eIF3h. *EMBO J.* **32**, 1087–1102 (2013).
66. C. F. Calkhoven, C. Müller, A. Leutz, Translational control of C/EBPalpha and C/EBPbeta isoform expression. *Genes Dev.* **14**, 1920–1932 (2000).
67. X. Pan, Y. Fang, X. Li, Y. Yang, H. B. Shen, RBPsuite: RNA-protein binding sites prediction suite based on deep learning. *BMC Genomics* **21**, 884 (2020).
68. M. H. G. Wiestler, "Insulin signaling and its role in Drosophila midgut homeostasis," Medizinischen Doktorgrades, Ruprecht Karls Universität (2015). https://www.ub.uni-heidelberg.de/archiv/20047. Accessed 11 October 2021.
69. A. Amcheslavsky, N. Ito, J. Jiang, Y. T. Ip, Tuberous sclerosis complex and Myc coordinate the growth and division of Drosophila intestinal stem cells. *J. Cell Biol.* **193**, 695–710 (2011).
70. J. K. Wen *et al.*, Atg9 antagonizes TOR signaling to regulate intestinal cell growth and epithelial homeostasis in *Drosophila*. *eLife* **6**, e29338 (2017).
71. D. Dutta *et al.*, Regional cell-specific transcriptome mapping reveals regulatory complexity in the adult Drosophila midgut. *Cell Rep.* **12**, 346–358 (2015).
72. C. Trapnell, L. Pachter, S. L. Salzberg, TopHat: Discovering splice junctions with RNA-Seq. *Bioinformatics* **25**, 1105–1111 (2009).
73. C. Trapnell *et al.*, Transcript assembly and quantification by RNA-Seq reveals unannotated transcripts and isoform switching during cell differentiation. *Nat. Biotechnol.* **28**, 511–515 (2010).